

RATIONAL SPECTRAL COLLOCATION METHOD FOR A COUPLED SYSTEM OF SINGULARLY PERTURBED BOUNDARY VALUE PROBLEMS*

Suqin Chen Yingwei Wang Xionghua Wu

Department of Mathematics, Tongji University, Shanghai 200092, China

Email: tjchensuqin@mail.tongji.edu.cn, wywshtj@gmail.com, wuxh@mail.tongji.edu.cn

Abstract

A novel collocation method for a coupled system of singularly perturbed linear equations is presented. This method is based on rational spectral collocation method in barycentric form with sinh transform. By sinh transform, the original Chebyshev points are mapped into the transformed ones clustered near the singular points of the solution. The results from asymptotic analysis about the singularity solution are employed to determine the parameters in this sinh transform. Numerical experiments are carried out to demonstrate the high accuracy and efficiency of our method.

Mathematics subject classification: 65L10, 65M70.

Key words: Singular perturbation, Coupled system, Rational spectral collocation method, Boundary layer, Reaction-diffusion, Convection-diffusion.

1. Introduction

In this paper, we consider a coupled system of $m \geq 2$ singularly perturbed linear equations in the unknown vector function $\mathbf{u} = (u_1, \dots, u_m)^T$. This system is coupled through its convective and reactive terms:

$$\mathcal{L} \mathbf{u} := -\varepsilon \mathbf{u}'' - B(x) \mathbf{u}' + A(x) \mathbf{u} = \mathbf{f}, \quad (1.1)$$

and it satisfies the boundary conditions

$$\mathbf{u}(0) = \mathbf{b}_0, \quad \mathbf{u}(1) = \mathbf{b}_1. \quad (1.2)$$

Here $A = (a_{ij})$ and $B = (b_{ij})$ are $m \times m$ matrices whose entries are assumed to lie in $C^2[0, 1]$, and $\varepsilon > 0$ is a small diffusion parameter whose presence makes the problem singularly perturbed. We assumed that $\mathbf{f} = (f_1, \dots, f_m)^T \in (C^2[0, 1])^m$, both $\mathbf{b}_0 = (b_{01}, \dots, b_{0m})^T$ and $\mathbf{b}_1 = (b_{11}, \dots, b_{1m})^T$ are constant vectors.

Coupled systems do appear in many applications, notably turbulent interaction of waves and currents [1], diffusion processes in electroanalytic chemistry [2], optimal control and certain resistance-capacitor electrical circuits [3], etc. Compared to single-equation singularly perturbed problems, coupled systems can model more complicated physical phenomena.

If $B \equiv 0$ in (1.1), the system is said to be of reaction-diffusion type. Shishkin [2] established finite difference method on a piecewise uniform mesh for the case $m = 2$; the results about the stability, convergence and error estimate for Shishkin's method, can be found in Madden [4], Lin β [5, 6], Matthews [7]. Stephens [8] proposed a parameter-uniform overlapping Schwarz

* Received June 11, 2010 / Revised version received November 11, 2010 / Accepted December 28, 2010 /
Published online June 27, 2011 /

method and Linβ [9] established a central difference scheme on certain layer-adapted meshes for the cases of $m \geq 2$. Generally speaking, the solution to the problem of this type has two boundary layers with width $\mathcal{O}(\sqrt{\varepsilon})$ respectively at $x = 0$ and $x = 1$ under some assumptions.

If $B \neq 0$, the system is said to be of convection-diffusion type. Riordan et al presented a finite difference method consisting of upwinding on piecewise-uniform Shishkin meshes for the cases of $m = 2$ [10] and $m > 2$ [11]. They also used a Jacobi-type iteration to compute the solution [12]. Generally speaking, the problem of this type has a solution with a single boundary layer of width $\mathcal{O}(\varepsilon)$ at $x = 0$ (or $x = 1$) under proper assumptions.

Furthermore, if (1.1) are coupled through their convective (first-order) terms (i.e. for each $i = 1, \dots, m$ there exists a $j \neq i$ such that $b_{ij} \neq 0$), we say it is strongly coupled; otherwise, if $B \equiv 0$ or B is just a non-zero diagonal matrix, it is said to be weakly coupled.

The spectral collocation method based on rational interpolants in barycentric form was proposed by Berrut and his collaborators [13–16]. An advantage of which is that after transform, the derivatives in underlying differential equation are not required to be transformed correspondingly as is usual in other methods. Besides, Tee and Trefethen [17] devised a sinh transform that maps original Chebyshev points clustered near the boundaries of $[-1, 1]$ into a new set of collocation points, say the transformed Chebyshev points, which are clustered near the singular point of a function. In order to determine the parameters in above sinh transform, singularities of the solution, including the location and width of the boundary layer, should be known. Hence, we resorted to the singularity location technique in asymptotic analysis and solved a parameterized singular perturbation problem [18].

Here we present a kind of numerical method based on rational spectral collocation in barycentric form with sinh transform (RSC-sinh method) for solving a coupled system of singularly perturbed problems in various types, both weakly coupled and strongly coupled. Numerical experiments illustrate that the RSC-sinh method enjoys improved spectral accuracy.

This paper is organized as follows. The asymptotic analysis of the problem is outlined in Section 2. In Section 3, we construct the RSC-sinh method for problem (1.1)-(1.2). The numerical results of several examples are given in Section 4. Finally, we present some concluding remarks in Section 5.

Notation. Through out this paper, C denotes a generic constant that may take different values at different places in our arguments. The definition of norm is:

- for a vector $\mathbf{y} = (y_0, \dots, y_m)^T$, $\|\mathbf{y}\| = \max_{p=0, \dots, m} |y_p|$;
- for a real-valued function $y \in C([0, 1])$, $\|y\|_{[0, 1]} = \max_{x \in [0, 1]} |y(x)|$;
- for a vector-valued function $\mathbf{z} = (z_0, \dots, z_m)^T$, $\|\mathbf{z}\|_{[0, 1]} = \max_{p=0, \dots, m} \|z_p\|_{[0, 1]}$.

2. Asymptotic Analysis

For the construction of RSC-sinh method, it is necessary to have properties of exact solution, especially the location and width of the boundary layer. The asymptotic analysis of problem (1.1) often involves a *Shishkin Decomposition* [19], which splits the solution into regular and layer components. It will be considered in reaction-diffusion case and convection-diffusion case respectively.

2.1. Weakly coupled system of reaction-diffusion problems

In this subsection, we consider the case $A \neq 0, B \equiv 0$ in (1.1), which is of reaction-diffusion type.

Assumption 2.1. A has positive diagonal entries and nonpositive off-diagonal entries, i.e.,

$$a_{ij} \begin{cases} > 0, & \text{if } i = j, \\ \leq 0, & \text{if } i \neq j. \end{cases}$$

Assumption 2.2. A is strictly diagonally dominant with $\sum_{k=1, k \neq i}^m |a_{ik}| < a_{ii}$ and $\sum_{j=1}^m a_{ij} > \alpha^2 > 0$, for $i = 1, \dots, m$.

Let \mathbf{v} and \mathbf{w} be the solutions of the boundary-value problems

$$\mathcal{L} \mathbf{v} = \mathbf{f}, \quad \mathbf{v}(0) = A(0)^{-1} \mathbf{f}(0), \quad \mathbf{v}(1) = A(1)^{-1} \mathbf{f}(1). \tag{2.1}$$

$$\mathcal{L} \mathbf{w} = \mathbf{0}, \quad \mathbf{w}(0) = \mathbf{b}_0 - \mathbf{v}(0), \quad \mathbf{w}(1) = \mathbf{b}_1 - \mathbf{v}(1). \tag{2.2}$$

Note that Assumption 2.2 implies the nonsingularity of matrix $A(x)$ for all $x \in [0, 1]$.

Lemma 2.1. Under Assumptions 2.1-2.2, \mathbf{v} and \mathbf{w} defined as (2.1) and (2.2) satisfy

$$\|\mathbf{v}^{(j)}\|_{[0,1]} \leq C (1 + (\sqrt{\varepsilon})^{2-j}),$$

and for $x \in [0, 1]$,

$$\|\mathbf{w}^{(j)}\|_{[0,1]} \leq C (\sqrt{\varepsilon})^{-j} \left(e^{-\alpha x / \sqrt{\varepsilon}} + e^{-\alpha(1-x) / \sqrt{\varepsilon}} \right),$$

for $j = 0, 1, 2$.

Proof. See [8, 9] for details. □

Theorem 2.1. If assumptions in Lemma 2.1 are satisfied, the solution to (1.1) and (1.2) has the following asymptotic expansion:

$$\mathbf{u}(x) = \mathbf{v}(x) + \tilde{\mathbf{w}}(x) + \mathcal{O}(\sqrt{\varepsilon}),$$

where

$$\tilde{\mathbf{w}}(x) = \begin{cases} \mathbf{w}(x), & x \in [0, x_*] \cup [1 - x_*, 1], \\ 0, & x \in [x_*, 1 - x_*], \end{cases} \quad 0 < x_* = -\frac{\ln \sqrt{\varepsilon}}{\alpha} \sqrt{\varepsilon} \ll 1. \tag{2.3}$$

Remark 2.1. The above theorem suggests that the solution \mathbf{u} has two boundary layer regions, $[0, x_*]$ and $[1 - x_*, 1]$, that is to say, the location of boundary layers are at the two endpoints of the underlying interval $[0, 1]$ and each of their width is $x_* = -\frac{\ln \sqrt{\varepsilon}}{\alpha} \sqrt{\varepsilon}$.

2.2. Strongly coupled system of convection-diffusion problem

In this subsection, we list an asymptotic analysis result of strongly coupled system of convection-diffusion problem.

Assumption 2.3. $B \neq 0$ is strictly diagonally dominant and hence invertible, and for $i = 1, \dots, m$, define $\beta_i := \min_{x \in [0,1]} b_{ii}(x) > 0$, $\beta = \min_i \beta_i$.

Note that each component u_i of the solution $\mathbf{u} = (u_1, \dots, u_m)^T$ will exhibit a boundary layer and the above assumption enables us to predict the layer in $u_i(x)$ will be at $x = 0$ [20].

Assumption 2.4. Diagonal entries of A satisfy $a_{ii}(x) \geq 0, \forall x \in [0, 1], i = 1, \dots, m$.

Assumption 2.5. The homogeneous reduced problem defined by $-B\hat{\mathbf{v}}' + A\hat{\mathbf{v}} = 0$, $\hat{\mathbf{v}}(1) = 0$, has only a trivial solution $\hat{\mathbf{v}} \equiv 0$.

Lemma 2.2. Let Assumptions 2.3 through 2.5 be satisfied. The regular component \mathbf{v} and layer component \mathbf{w} defined in [11] satisfy

$$\|\mathbf{v}^{(j)}\|_{[0,1]} \leq C(1 + \varepsilon^{2-j}),$$

and for $x \in [0, 1]$

$$\|\mathbf{w}_i^{(j)}\|_{[0,1]} \leq C \varepsilon^{-j} e^{-\beta x/\varepsilon},$$

for $j = 0, 1, 2$ and $i = 1, \dots, m$.

Proof. See [7, 11] for details. □

Theorem 2.2. If assumptions in Lemma 2.2 are satisfied, the solution of (1.1) and (1.2) has the following asymptotic expansion:

$$\mathbf{u}(x) = \mathbf{v}(x) + \tilde{\mathbf{w}}(x) + \mathcal{O}(\varepsilon),$$

where

$$\tilde{\mathbf{w}}(x) = \begin{cases} \mathbf{w}(x), & x \in [0, x_*], \\ 0, & x \in [x_*, 1], \end{cases} \quad 0 < x_* = -\frac{\ln \varepsilon}{\beta} \varepsilon \ll 1. \quad (2.4)$$

Remark 2.2. The above theorem suggests that the boundary layer region of the solution \mathbf{u} is $[0, x_*]$, that is to say, the location of boundary layer is at the left endpoint of the underlying interval $[0, 1]$ and its width is $x_* = -\frac{\ln \varepsilon}{\beta} \varepsilon$.

3. RSC-sinh Method

3.1. The rational interpolation in barycentric form [16]

The barycentric form of a rational function $p_N(x)$ which interpolates the function $u(x)$ at the points $\{x_k\}$ is

$$p_N(x) = \frac{\sum_{k=0}^N \frac{\omega_k}{x-x_k} u(x_k)}{\sum_{k=0}^N \frac{\omega_k}{x-x_k}}, \quad (3.1)$$

where the barycentric weights $\{\omega_k\}_{k=0}^N$ are chosen as $\omega_0 = \frac{1}{2}, \omega_N = \frac{(-1)^N}{2}, \omega_k = (-1)^k, k = 1, \dots, N-1$ when $\{x_k\}_{k=0}^N$ are Chebyshev points.

The rational interpolation based on barycentric form with transformed Chebyshev points has the following convergence analysis.

Theorem 3.1. ([14]) *Let D_1, D_2 be domains in \mathbb{C} containing $J = [-1, 1]$ and a real interval I respectively. Let $g : D_1 \mapsto D_2$ be a conformal map such that $g(J) = I$. If $u : D_2 \mapsto \mathbb{C}$ is a function such that the composition $u \circ g : D_1 \mapsto \mathbb{C}$ is analytic inside and on an ellipse E_ρ , with foci at ± 1 and the sum of its semi-major axis length and semi-minor axis length equal to $\rho > 1$. Let $p_N(x)$ be rational function (3.1) interpolating u between transformed Chebyshev points $\hat{x}_k = g(\cos(k\pi/N))$ with barycentric weights. For $\forall x \in [-1, 1]$,*

$$|p_N(x) - u(x)| = \mathcal{O}(\rho^{-N}).$$

Remark 3.1. Theorem 3.1 suggests that one should choose a conformal map g so that the ellipse of analyticity of $u \circ g$ is larger than one of u , and apply g in a spectral method based on rational interpolant of the form (3.1), to obtain an approximation of u which is more accurate than that obtained using the Chebyshev spectral method with the same number of grid points. Two kinds of g will be considered in next subsection designed for the problem with single boundary layer and two boundary layers respectively.

The derivatives of function $u(x)$ at the points $\{\hat{x}_k\}_{k=0}^N$ can be evaluated as the product of differentiation matrices and data vectors, as common spectral collocation method does. An advantage of the barycentric rational interpolation is the simplicity of its derivatives formulae at \hat{x}_j . The n th derivative of $p_N(x)$ evaluated at \hat{x}_j can be written in the form $p_N^{(n)}(\hat{x}_j) = \sum_{k=0}^N D_{jk}^{(n)} u(\hat{x}_k)$, where the first and second order differentiation matrices, $D^{(1)}$ and $D^{(2)}$, are given by

$$D_{jk}^{(1)} = \begin{cases} \frac{\omega_k}{\omega_j(\hat{x}_j - \hat{x}_k)}, & j \neq k \\ -\sum_{i \neq j} D_{ji}^{(1)}, & j = k \end{cases} \tag{3.2}$$

$$D_{jk}^{(2)} = \begin{cases} 2D_{jk}^{(1)} \left(D_{jj}^{(1)} - \frac{1}{\hat{x}_j - \hat{x}_k} \right), & j \neq k \\ -\sum_{i \neq j} D_{ji}^{(2)}, & j = k. \end{cases} \tag{3.3}$$

Note that differentiation matrices (3.2) and (3.3) only rely on weights ω_k and new points \hat{x}_k , which is the reason why the underlying equation doesn't require to be transformed into new coordinates after maps shown in next subsection.

3.2. The sinh transform

In a rational spectral collocation method, the space interval of the problem considered is usually assumed to be $[-1, 1]$. By introducing the transform $x = 0.5(y+1)$, $x \in [0, 1]$, $y \in [-1, 1]$ and defining $\hat{u}(y) = u(x) = u(0.5(y+1))$, then $u'(x) = 2\hat{u}'(y)$, $u''(x) = 4\hat{u}''(y)$ and (1.1) is converted to the following problem:

$$-4\varepsilon\hat{u}''(y) - 2B\hat{u}'(y) + A\hat{u}(y) = \hat{\mathbf{f}}(y), \tag{3.4}$$

$$\hat{\mathbf{u}}(-1) = \mathbf{b}_0, \quad \hat{\mathbf{u}}(1) = \mathbf{b}_1. \tag{3.5}$$

The original Chebyshev points are

$$x_k = \cos(k\pi/N) \in [-1, 1], \quad k = 0, 1, \dots, N.$$

These points are clustered near the boundaries of $[-1,1]$.

However, what we seek is a set of points that are denser inside the boundary layer region than outside. For the case that u has a single boundary layer at $x = \lambda$ with width δ , Tee [17] chose a conformal map g expressed by sinh transform:

$$g_{\lambda,\delta}(x) = \lambda + \delta \sinh \left[\sinh^{-1} \left(\frac{1+\lambda}{\delta} \right) \frac{x-1}{2} + \sinh^{-1} \left(\frac{1-\lambda}{\delta} \right) \frac{x+1}{2} \right]. \quad (3.6)$$

Transformed Chebyshev points $\{g_{\lambda,\delta}(x_k)\}_{k=0}^N$ are clustered near the location of boundary layer $x = \lambda$ and their density is determined by the boundary layer width δ . The thinner the boundary layer, the denser points.

According to Remark 2.2, if (3.4) is of convection-diffusion type, parameters in (3.6) should be chosen as

$$\lambda = -1, \delta = -2 \frac{\ln \varepsilon}{\beta} \varepsilon. \quad (3.7)$$

In order to deal with problems with two boundary layers, motivated by the work of Tee, we define the combined sinh transform as

$$\tilde{g}_\delta(x) = \begin{cases} \frac{1}{2} [g_{-1,\delta}(2x+1) - 1], & x \in [-1, 0), \\ \frac{1}{2} [g_{1,\delta}(2x-1) + 1], & x \in [0, 1]. \end{cases} \quad (3.8)$$

All derivatives of the piecewise map \tilde{g} at $x = 0$ are continuous so that the spectral accuracy could be preserved. If (3.4) is of reaction-diffusion type, according to Remark 2.1, the parameter in (3.8) should be chosen as

$$\delta = -2 \frac{\ln \sqrt{\varepsilon}}{\alpha} \sqrt{\varepsilon}. \quad (3.9)$$

3.3. Numerical algorithm

To show RSC-sinh method in detailed algorithm, we take the singularly perturbed problem of convection-diffusion type for example. Let transformed Chebyshev collocation points be

$$Y = \{y_k\}_{k=0}^N = \{g_{\lambda,\delta}(\cos(k\pi/N))\}_{k=0}^N, \quad (3.10)$$

where $g_{\lambda,\delta}$ is expressed by (3.6) in which $\lambda = -1, \delta = -2 \frac{\ln \varepsilon}{\beta} \varepsilon$.

Evaluating equations in (3.4) at points $y_k, k = 0, \dots, N$ yields

$$\left(-4\varepsilon I \otimes D^{(2)} - 2B \otimes D^{(1)} + A \otimes I \right) \mathbf{U} = \mathbf{F}, \quad (3.11)$$

where

$$\mathbf{U} = \begin{bmatrix} \hat{\mathbf{u}}_1(Y) \\ \hat{\mathbf{u}}_2(Y) \\ \dots \\ \hat{\mathbf{u}}_m(Y) \end{bmatrix}, \quad \hat{\mathbf{u}}_i(Y) = \begin{bmatrix} \hat{u}_i(y_0) \\ \hat{u}_i(y_1) \\ \dots \\ \hat{u}_i(y_N) \end{bmatrix}, \quad \mathbf{F} = \begin{bmatrix} \hat{\mathbf{f}}_1(Y) \\ \hat{\mathbf{f}}_2(Y) \\ \dots \\ \hat{\mathbf{f}}_m(Y) \end{bmatrix}, \quad \hat{\mathbf{f}}_i(Y) = \begin{bmatrix} \hat{f}_i(y_0) \\ \hat{f}_i(y_1) \\ \dots \\ \hat{f}_i(y_N) \end{bmatrix},$$

for $i = 1, \dots, m$, \otimes is Kronecker product.

Boundary conditions in (3.5) suggest that

$$\hat{u}_i(y_0) = b_{0i}, \quad \hat{u}_i(y_N) = b_{1i}, \quad i = 1, \dots, m. \quad (3.12)$$

Solving the linear algebra system including (3.11) and (3.12), we can obtain the numerical solution of (3.4) and (3.5).

Remark 3.2. If the singularly perturbed problem (3.4) is of reaction-diffusion type, then we use transformed Chebyshev collocation points as

$$Y = \{y_k\}_{k=0}^N = \left\{ \tilde{g}_\delta \left(\cos \left(\frac{k\pi}{N} \right) \right) \right\}_{k=0}^N, \tag{3.13}$$

where \tilde{g}_δ is expressed by (3.8) in which $\delta = -2\frac{\ln\sqrt{\varepsilon}}{\alpha}\sqrt{\varepsilon}$.

4. Numerical Experiments

Consider other two kinds of spectral methods combined with suitable transformation proposed by Tao Tang et al. for solving singularly perturbed problems. One family is Legendre-Galerkin method (PLGM) with transformation [21]:

$$x^t = g_k(x) = -1 + \kappa \int_{-1}^x (1 - \eta^2)^k d\eta, \quad k \geq 1, \quad \text{and } \kappa = \frac{2}{\int_{-1}^1 (1 - \eta^2)^k d\eta}. \tag{4.1}$$

Another family is the boundary layer resolving Chebyshev collocation method (BLRCC) with the transformation $x^t = g_m(x)$ [22] where

$$g_0(x) = x, \quad g_m(x) = \sin \left(\frac{\pi}{2} g_{m-1}(x) \right), \quad m \geq 1. \tag{4.2}$$

In (4.1) and (4.2), x is the original variable (i.e. original Chebyshev points) and x^t is the transformed variable (i.e. transformed Chebyshev points); $k, m = 1, 2$.

To demonstrate the high accuracy and efficiency of our method, we will employ the conventional Chebyshev collocation method (CCC), PLGM, BLRCC and RSC-sinh method to solve problems with exact solutions (Example 4.1 and 4.2) respectively and compare results. Example 4.3 and 4.4 are problems with variable coefficients.

Example 4.1. Consider the reaction-diffusion problem with constant coefficients: [5]

$$B = 0, \quad A = \begin{pmatrix} 2 & -1 \\ -1 & 2 \end{pmatrix}, \quad \mathbf{f} = \mathbf{A} = \begin{pmatrix} 1 \\ 2 \end{pmatrix}, \quad \mathbf{b}_0 = \mathbf{b}_1 = \mathbf{A} = \begin{pmatrix} 0 \\ 0 \end{pmatrix}.$$

The exact solution of this problem is

$$\mathbf{u} = \frac{1}{2} (1, 1)^T y_1 + \frac{1}{2} (-1, 1)^T y_2,$$

where

$$y_1 = 3 \frac{e^{(x-2)/\sqrt{\varepsilon}} - e^{-x/\sqrt{\varepsilon}} - e^{(x-1)/\sqrt{\varepsilon}} + e^{-(x+1)/\sqrt{\varepsilon}}}{1 - e^{-2/\sqrt{\varepsilon}}} + 3,$$

$$y_2 = \frac{1}{3} \frac{e^{\sqrt{3}(x-2)/\sqrt{\varepsilon}} - e^{-\sqrt{3}x/\sqrt{\varepsilon}} - e^{\sqrt{3}(x-1)/\sqrt{\varepsilon}} + e^{-\sqrt{3}(x+1)/\sqrt{\varepsilon}}}{1 - e^{-2\sqrt{3}/\sqrt{\varepsilon}}} + \frac{1}{3}.$$

Table 4.1: The maximum error of RSC-sinh method in Example 4.1 with various ε .

N	ε			
	10^{-14}	10^{-18}	10^{-22}	10^{-26}
64	8.9234×10^{-6}	3.1036×10^{-4}	1.7980×10^{-3}	4.2363×10^{-3}
96	2.3133×10^{-9}	1.2332×10^{-6}	4.2591×10^{-5}	3.3898×10^{-4}
128	7.9462×10^{-11}	6.4827×10^{-9}	3.5721×10^{-7}	1.3284×10^{-5}

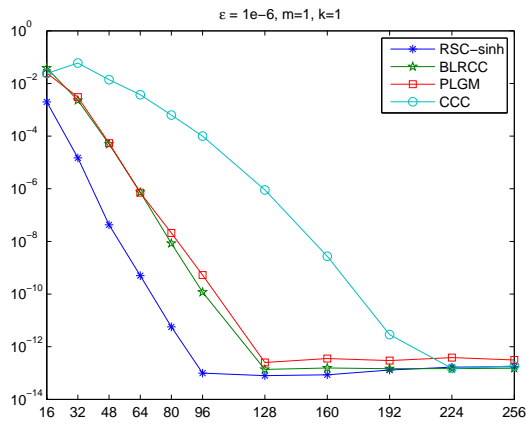


Fig. 4.1. Exponential rates of convergence of Example 4.1 when $\varepsilon = 10^{-6}$.

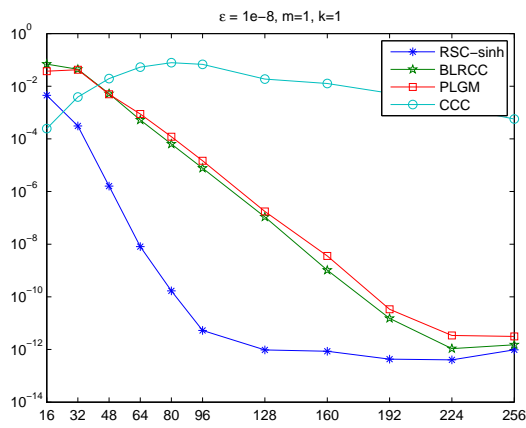


Fig. 4.2. Exponential rates of convergence of Example 4.1 when $\varepsilon = 10^{-8}$.

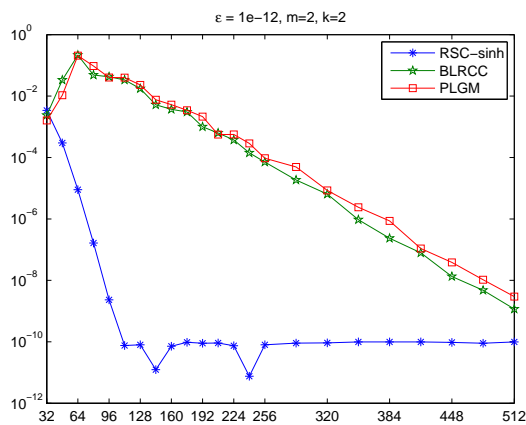


Fig. 4.3. Exponential rates of convergence of Example 4.1 when $\varepsilon = 10^{-12}$.

In RSC-sinh method, we use the transform (3.8) and parameters are chosen as (3.9) in which $\alpha = 0.99$.

In Figs. 4.1–4.3, we plot the maximum errors on a semi-log scale, in the cases with $\varepsilon = 10^{-6}, 10^{-8}, 10^{-12}$ respectively. These figures show that all of the transformation (3.8), (4.1) and (4.2) could speed up the spectral convergence, but the RSC-sinh method is able to achieve higher accuracy while using fewer points.

Fig. 4.4 shows the numerical solutions obtained by CCC, BLRCC and RSC-sinh approaches respectively. There are more points located in the boundary layer region in the case of RSC-sinh than other cases, though the numbers of total collocation points in the three methods are the same, $N = 64$. Fig. 4.5 shows the point-wise errors, from which we can observe that the maximum error occurs in the boundary layer regions.

For the cases with $10^{-12} \leq \varepsilon \leq 1$, the maximum error of finite difference method with Shishkin meshes [5] is $\eta^N = 2.682 \times 10^{-3}$ when $N = 128$. Table 4.1 lists the maximum errors of the cases with much thinner layers, some of which are not considered in [5].

In order to find how the selection of sinh-transform parameter α affects computing results,

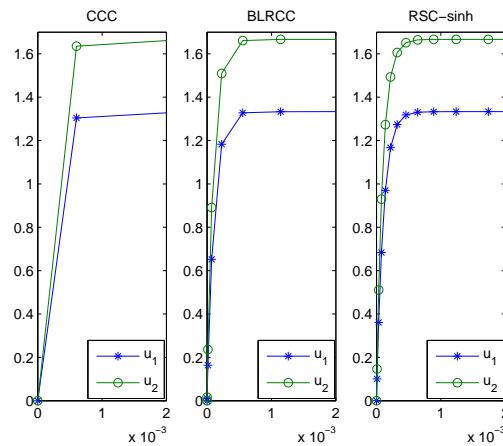


Fig. 4.4. Numerical solutions of Example 4.1 near left boundary region with $\varepsilon = 10^{-8}$, $N = 64$.

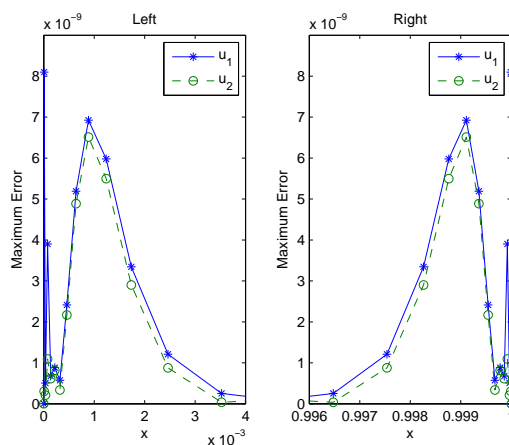


Fig. 4.5. Pointwise errors of Example 4.1 near boundary region with $\varepsilon = 10^{-8}$, $N = 64$.

further computing of Example 4.1 for different α has been implemented. The results are showed in Fig. 4.6, from which we can observe that the minimum error occurs at $\alpha = 1$; when $\alpha \leq 1$, errors decrease rapidly with α ; when $\alpha > 1$, errors increase slowly with α .

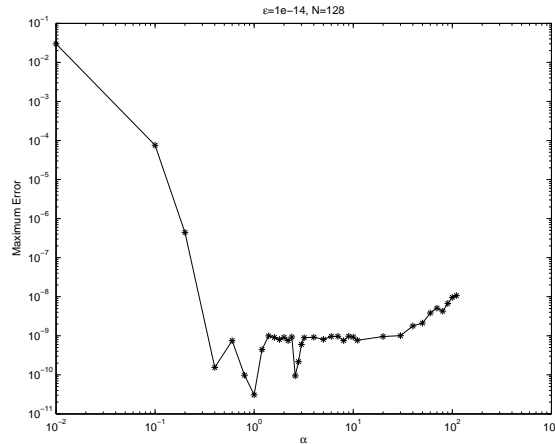


Fig. 4.6. Maximum errors of Example 4.1 with $\varepsilon = 10^{-14}$, $N = 128$ for different α .

Example 4.2. Consider the convection-diffusion problem with constant coefficients: [11, 12]

$$B = \begin{pmatrix} 3 & -1 & -1 \\ -1 & 4 & -2 \\ -1 & -2 & 4 \end{pmatrix}, \quad A = 0, \quad \mathbf{f} = \begin{pmatrix} -4 \\ 11 \\ -7 \end{pmatrix},$$

$$\mathbf{b}_0 = \begin{pmatrix} -1 \\ 4 \\ -1 \end{pmatrix}, \quad \mathbf{b}_1 = \begin{pmatrix} e^{-1/\varepsilon} - 2e^{-4/\varepsilon} + 1 \\ e^{-1/\varepsilon} + e^{-4/\varepsilon} + 2e^{-6/\varepsilon} - 2 \\ e^{-1/\varepsilon} + e^{-4/\varepsilon} - 2e^{-6/\varepsilon} \end{pmatrix}.$$

The exact solution of this problem is

$$\mathbf{u} = (1, 1, 1)^T e^{-x/\varepsilon} + (-2, 1, 1)^T e^{-4x/\varepsilon} + (0, 2, -2)^T e^{-6x/\varepsilon} + (x, -2x, x - 1)^T.$$

The parameters in transform (3.6) are chosen as (3.7) in which $\beta = 2.55$.

In Figs. 4.7–4.8, we plot the maximum errors on a semi-log scale, in the cases with $\varepsilon = 10^{-3}, 10^{-6}$ respectively. Fig. 4.9 and Fig. 4.10 show the numerical solutions and point-wise errors in the boundary layer region respectively. These figures illustrate that RSC-sinh method perform better than the spectral methods in [21, 22].

The maximum error for the case with $\varepsilon = 2^{-12}$ obtained by piecewise-uniform Shishkin mesh combined with Jacobi-type iteration [12] is 3.917×10^{-2} when $N = 1024$; the maximum

Table 4.2: The maximum error of RSC-sinh method in Example 4.2 with various ε .

N	ε			
	10^{-6}	10^{-7}	10^{-8}	10^{-9}
96	2.308×10^{-7}	1.3887×10^{-4}	1.7094×10^{-2}	9.1648×10^{-1}
128	1.4722×10^{-8}	1.0556×10^{-7}	6.2019×10^{-5}	1.2265×10^{-3}
160	3.3384×10^{-9}	2.8279×10^{-7}	1.8418×10^{-6}	2.9805×10^{-4}
192	1.7134×10^{-9}	1.3868×10^{-7}	9.8919×10^{-7}	1.2304×10^{-4}

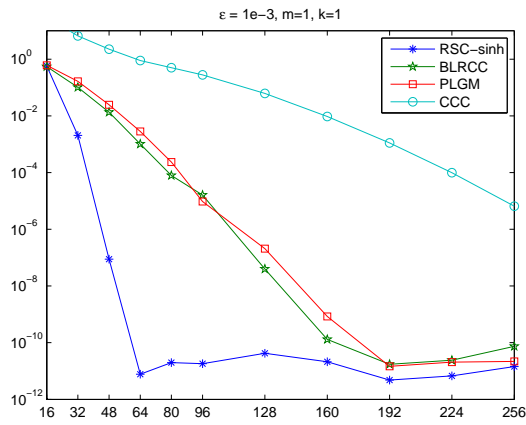


Fig. 4.7. Exponential rates of convergence of Example 4.2 when $\varepsilon = 10^{-3}$.

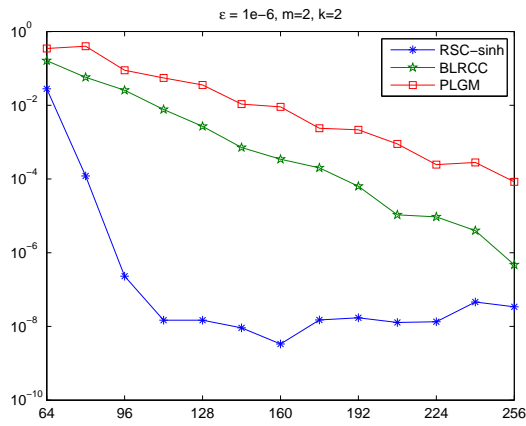


Fig. 4.8. Exponential rates of convergence of Example 4.2 when $\varepsilon = 10^{-6}$.

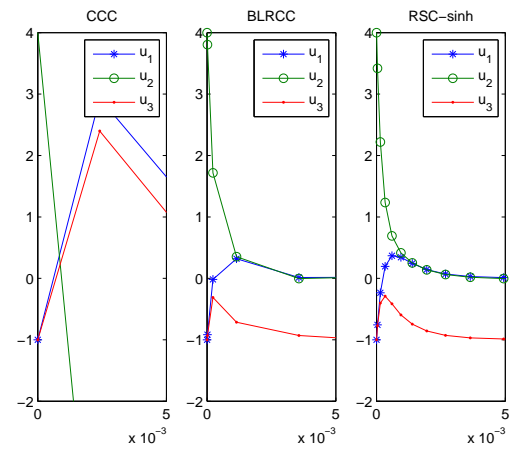


Fig. 4.9. Numerical solutions of Example 4.2 near boundary region with $\varepsilon = 10^{-3}$, $N = 64$.

error for the case with $\varepsilon = 10^{-7}$ obtained by the method consisting of upwinding on piecewise uniform Shishkin meshes [11] is 1.472×10^{-2} when $N = 1024$. Table 4.2 lists the maximum errors of the RSC-sinh method for $\varepsilon = 10^{-6}, 10^{-7}, 10^{-8}, 10^{-9}$.

About the selection of sinh-transform parameter β , further computing of Example 4.2 for different β has been implemented. The results are showed in Fig. 4.11, from which we can observe that the minimum error occurs at $\beta = 2.55$; when $\beta \leq 2.55$, errors decrease rapidly with β ; when $\beta > 2.55$, errors decrease slowly with β .

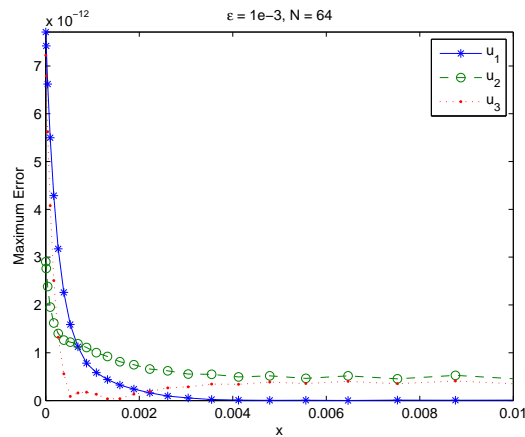


Fig. 4.10. Pointwise errors of Example 4.2 near boundary region with $\varepsilon = 10^{-3}$, $N = 64$.

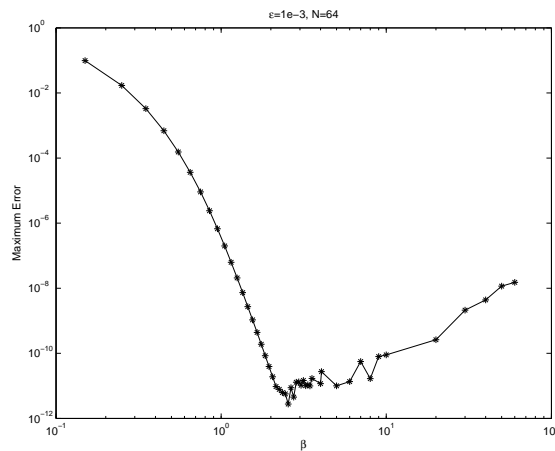


Fig. 4.11. Maximum errors of Example 4.2 with $\varepsilon = 10^{-3}$, $N = 64$ for different β .

Example 4.3. Consider the convection-diffusion problem with variable coefficients: [10]

$$B = \begin{pmatrix} 4 + xe^x & -1 - 2x \\ -1 - x & 2 + x^2 \end{pmatrix}, \quad A = 0, \quad \mathbf{f} = \begin{pmatrix} 1 + x + 3x^2 \\ 2x - 1 \end{pmatrix}, \quad \mathbf{b}_0 = \begin{pmatrix} 2 \\ 1 \end{pmatrix}, \quad \mathbf{b}_1 = \begin{pmatrix} 2 \\ 2 \end{pmatrix}.$$

In the transform (3.6), the parameters are chosen as (3.7) where β is chosen as 1.99. The exact solution to this problem is unknown. Fig. 4.12 displays the plot of numerical solution for $\varepsilon = 10^{-2}, N = 24$, which is the same as the figure in [10] with 32 points.

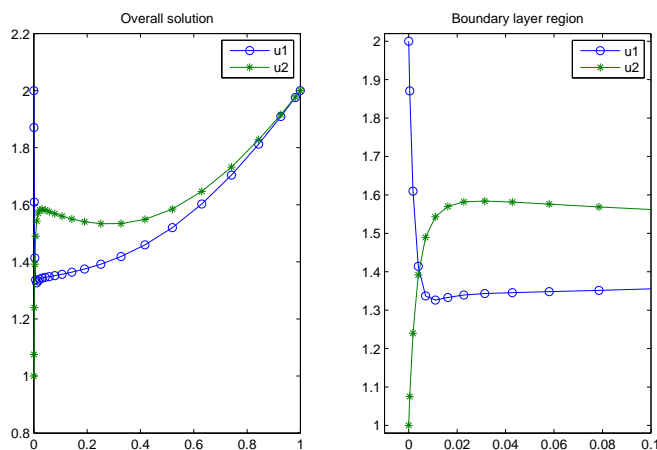


Fig. 4.12. Numerical results of Example 4.3 with $\varepsilon = 10^{-2}$, $N = 24$.

Example 4.4. Consider the reaction-diffusion problem with variable coefficients [8]

$$B = 0, \quad A = \begin{pmatrix} 2(x+1)^2 & -(1+x^3) & -0.1 & -0.2 \\ -2\cos(\frac{\pi x}{4}) & (1+\sqrt{2})e^{1-x} & -0.2 & -0.1 \\ -2\cos(\frac{\pi x}{4}) & -\frac{1}{2}(x+1)^2 & 2(1+\sqrt{2})e^{1-x} & -\cos(\frac{\pi}{5}) \\ -(1+x^3) & -0.1 & -0.2 & 3(x+1)^3 \end{pmatrix},$$

$$\mathbf{f} = \begin{pmatrix} 2+x \\ 1 \\ 2e^x \\ 0.1 \end{pmatrix}, \quad \mathbf{b}_0 = \mathbf{b}_1 = \begin{pmatrix} 0 \\ 0 \\ 1 \\ 2 \end{pmatrix}.$$

The exact solution to this problem is unknown. Figs. 4.13–4.14 displays the plot of numerical solution for $\varepsilon = 2^{-20}$, $N = 128$, using the transform (3.8) and (3.9) with $\alpha = 1.99$.

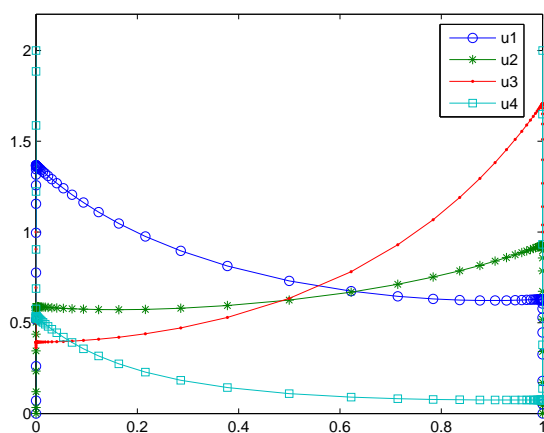


Fig. 4.13. The overall solution of Example 4.4 with $\varepsilon = 2^{-20} \approx 10^{-6}$, $N = 128$.

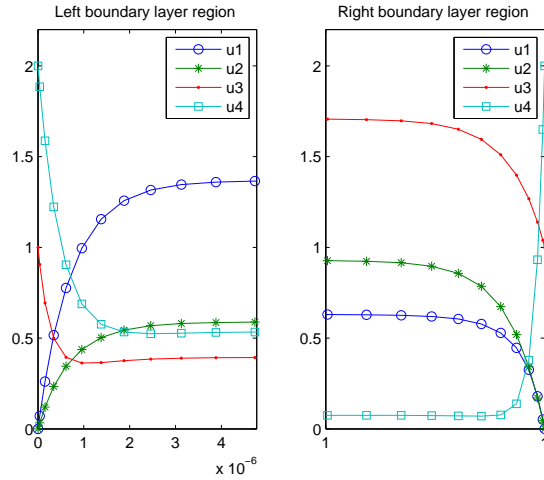


Fig. 4.14. The boundary layer regions of Example 4.4 with $\epsilon = 2^{-20}$, $N = 128$.

5. Conclusions

A novel collocation method, named RSC-sinh, has been developed for solving the singularly perturbed problem. The key to the success of this method is to apply the results from asymptotic analysis to the sinh transformation. The details of the numerical algorithms show that our method is very easy to use and ready for computer implementation.

Numerical experiments justify that compared to classic spectral method with other transformations, the present RSC-sinh has the following advantages:

1. The transformed collocation points in RSC-sinh are clustered near the location of boundary layer(s), which leads to higher accuracy but using fewer points in solving both reaction-diffusion and convection-diffusion problems.
2. Since the RSC-sinh method is based on rational interpolants in barycentric form, after transformation, the derivatives in the underlying differential equation do not require to be transformed correspondingly as is usual in other methods.

Regarding to the comparison between spectral methods with transformation and other methods with ϵ -uniform meshes, we make some remarks here:

1. Spectral methods have the advantage that the exponential rate of convergence can be obtained. The spectral methods plus coordinate stretching allow us to use reasonably large N to gain the exponential rate of convergence. To discuss the computational effort, we introduce the computational complexity, i.e. the total amount of work required to achieve a solution accurate to within ϵ . Since the finite difference methods can achieve an $\epsilon = \mathcal{O}(N_d^{-2})$ error by using N_d points while require $\mathcal{O}(N_d)$ operations, its computational complexity is $\mathcal{O}(\epsilon^{-\frac{1}{2}})$; For the spectral-type methods, the error is $\epsilon = \mathcal{O}(e^{-N_s})$ and need $\mathcal{O}(N_s^3)$ operations at most, so its computational complexity is $\mathcal{O}(\ln^3(\frac{1}{\epsilon}))$.
2. Spectral methods are not appropriate if one is interested in details of arbitrarily thin boundary layers because in practice it is essentially impossible to resolve arbitrarily thin boundary layers with a non-adaptive ϵ -independent coordinate stretching [21]. To fully

resolve an arbitrarily small boundary layers, ε -uniform meshes such as Shishkins grid [2] and Schwab and Suris grid [23] should be employed.

In the future work, we expect to expand our method to time-dependant systems.

Acknowledgments. The support from the National Natural Science Foundation of China under Grants No.10671146 and No.50678122 is acknowledged. The authors are grateful to the referee and the editor for helpful comments and suggestions.

References

- [1] G.P. Thomas, Towards an improved turbulence model for wave-current interactions, *Second Annual Report to EU MAST-III Project "The Kinematics and Dynamics of Wave-Current Interactions"*, 1998.
- [2] G.I. Shishkin, Mesh approximation of singularly perturbed boundary-value problems for systems of elliptic and parabolic equations, *Comp. Maths. Math. Phys.*, **35** (1995), 429-446.
- [3] P.V. Kokotović, Applications of singular perturbation techniques to control problems, *SIAM Rev.*, **26** (1984), 501-550.
- [4] N. Madden and M. Stynes, A uniformly convergent numerical method for a coupled system of two singularly perturbed linear reaction-diffusion problems, *IMA J. Numer. Anal.*, **23**, 2003, 627-644.
- [5] T. Linß and N. Madden, An improved error estimate for a numerical method for a system of coupled singularly perturbed reaction-diffusion equations, *Comput. Method. Appl. M.*, **3**, 2003, 417-423.
- [6] T. Linß and N. Madden, Accurate solution of a system of coupled singularly perturbed reaction-diffusion equations, *Computing*, **3**, 2004, 121-133.
- [7] S. Matthews, E. O'Riordan and G.I. Shishkin, A numerical method for a system of singularly perturbed reaction-diffusion equations, *J. Comput. Appl. Math.*, **145** (2002), 151-166.
- [8] M. Stephens and N. Madden, A parameter-uniform Schwarz method for a coupled system of reaction-diffusion equations, *J. Comput. Appl. Math.*, **230** (2009), 360-370.
- [9] T. Linß and N. Madden, Layer-adapted meshes for a linear system of coupled singularly perturbed reaction-diffusion problems, *IMA J. Numer. Anal.*, **29** (2009), 109-125.
- [10] E. O'Riordan and M. Stynes, Numerical analysis of a strongly coupled system of two singularly perturbed convection-diffusion problems, *Adv. Comput. Math.*, **30** (2009), 101-121.
- [11] E. O'Riordan and J. Stynes and M. Stynes, A parameter-uniform finite difference method for a coupled system of convection-diffusion two-point boundary value problems, *Numer. Math. Theor. Meth. Appl.*, **1** (2008), 176-197.
- [12] E. O'Riordan and J. Stynes and M. Stynes, An iterative numerical algorithm for a strongly coupled system of singularly perturbed convection-diffusion problems, in *NAA 2008, LNCS 5434*, Springer-Verlag, Berlin Heidelberg, 2009, 104-115.
- [13] R. Baltensperger and J.P. Berrut and Y. Dubey, The linear rational pseudospectral method with preassigned poles, *Numer. Algorithms*, **33** (2003), 53-63.
- [14] R. Baltensperger and J.P. Berrut and B. Noël, Exponential convergence of a linear rational interpolant between transformed Chebyshev points, *Math. Comput.*, **68** (1999), 1109-1120.
- [15] J.P. Berrut and L.N. Trefethen, Barycentric Lagrange interpolation, in *Trends and Applications in Constructive Approximation*, *SIAM Rev.*, **46** (2004), 501-517.
- [16] J.P. Berrut and R. Baltensperger and H.D. Mittelmann, Recent development in barycentric rational interpolation, in *Trends and Applications in Constructive Approximation*, *Internat. Ser. Numer. Math.*, **15** (2005), 27-51.
- [17] T.W. Tee and L.N. Trefethen, A rational spectral collocation method with adaptively transformed Chebyshev grid points, *SIAM J. Sci. Comput.*, **28** (2006), 1798-1811.

- [18] Y. Wang, S. Chen and X. Wu, A rational spectral collocation method for solving a class of parameterized singular perturbation problems, *J. Comput. Appl. Math.*, **233** (2010), 2652-2660.
- [19] J.J.H. Miller and E. O'Riordan and G.I. Shishkin, Fitted Numerical Methods for Singular Perturbation Problems-Error Estimates in the Maximum Norm for Linear Problems in One and Two Dimensions, World Scientific, Singapore, 1996.
- [20] H.G. Roos and M. Stynes and L. Tobiska, Robust Numerical methods for singularly perturbed differential equations, Springer-Verlag, Berlin Heidelberg New York, 1996.
- [21] W. Liu and T. Tang, Error analysis for a Galerkin-spectral method with coordinate transformation for solving singularly perturbed problems, *Appl. Numer. Math.*, **38** (2001), 315-345.
- [22] T. Tang and M. R. Trummer, Boundary layer resolving pseudospectral methods for singular perturbation problems, *Appl. Numer. Math.*, **17** (1996), 430-438.
- [23] C. Schwab and M. Suri, The p and hp versions of the finite element method for problems with boundary layers, *Math. Comput.*, **65** (1996), 1403-1429.